

Transfer-matrix approach to three-dimensional bond percolation: An application of Novotny's formalism

Yoshihiro Nishiyama

Department of Physics, Faculty of Science, Okayama University, Okayama 700-8530, Japan

(Received 5 October 2005; published 12 January 2006)

A transfer-matrix simulation scheme for the three-dimensional ($d=3$) bond percolation is presented. Our scheme is based on Novotny's transfer-matrix formalism, which enables us to consider arbitrary (integral) number of sites N constituting a unit of the transfer-matrix slice even for $d=3$. Such an arbitrariness allows us to perform systematic finite-size-scaling analysis of the criticality at the percolation threshold. Diagonalizing the transfer matrix for $N=4,5,\dots,10$, we obtain an estimate for the correlation-length critical exponent $\nu=0.81(5)$.

DOI: [10.1103/PhysRevE.73.016114](https://doi.org/10.1103/PhysRevE.73.016114)

PACS number(s): 64.60.Ak, 05.10.-a, 05.70.Jk, 75.40.Mg

I. INTRODUCTION

The transfer-matrix method has an advantage over the Monte Carlo method in that it provides information free from the statistical (sampling) error and the problem of slow relaxation to thermal equilibrium. On one hand, the tractable system size is severely limited, because the transfer-matrix size increases exponentially as the system size enlarges. Such a difficulty could be even more serious for "geometrical" problems such as the percolation, for which the configuration space is much larger than that of the Ising model, for example.

A transfer-matrix approach to the percolation in two dimensions ($d=2$) was discussed by Derrida and Vannimenus [1]. They treated the system sizes (transfer-matrix strip widths) up to $N=5$. Performing an extensive phenomenological renormalization group (finite-size-scaling) analysis [2], they estimated the correlation-length critical exponent as $\nu=1.2\sim 1.4$; the variance is due to the choice of the boundary conditions. Their result is quite consistent with the exact value $\nu=4/3$, indicating that the transfer-matrix approach to percolation would be promising. Because the transfer-matrix data are free from the statistical error, the data allow us to take its numerical derivative, which provides valuable information as to the subsequent finite-size-scaling analysis.

It turned out, however, that its naive extension to the $d=3$ case is rather problematic; we refer to Sec. 4.4 of Ref. [3] for an overview. Actually, for $d=3$, as the system size (linear dimension) L enlarges, the number of constituent sites $N(=L^2)$ of the transfer-matrix unit soon exceeds the limit of the available computer resources.

The aim of this paper is to develop an improved version of the transfer-matrix formalism for the $d=3$ bond percolation. For that purpose, we utilize Novotny's idea, which has been applied successfully to various Ising models in $d\leq 7$ [4–9]. His formalism stems on a very formal expression for the transfer-matrix elements. It enables us to consider arbitrary (integral) number of constituent sites $\forall N$ even for $d\geq 3$. Owing to this arbitrariness, we are able to treat a variety of system sizes and perform systematic finite-size-scaling analysis of the numerical data. In this paper, we demonstrate that his idea is applicable to the $d=3$ bond percolation.

The rest of this paper is organized as follows. In Sec. II, we formulate the transfer-matrix scheme for the $d=3$ bond percolation. We place an emphasis how we adapted Novotny's idea to the bond-percolation problem. The simulation results are shown in Sec. III. Taking an advantage that we can treat various system sizes, we manage the phenomenological renormalization group [2] (finite-size-scaling) analysis. Thereby, we obtain an estimate for the correlation-length critical exponent $\nu=0.81(5)$. In Sec. IV, we present the summary and discussions.

II. CONSTRUCTION OF THE TRANSFER MATRIX FOR THE THREE-DIMENSIONAL BOND PERCOLATION

In this section, we set up the transfer-matrix formalism for the $d=3$ bond percolation. As mentioned in the introduction, we adopt Novotny's idea [4]. So far, his idea has been applied to various types of the Ising models in $d\leq 7$. Here, we show that his idea is also applicable to the bond percolation. At the end of this section, we argue a conceptual difference from the original Novotny method.

A. Configuration space

Above all, we need to set up the configuration space so as to represent the transfer-matrix elements explicitly. The bases of the configuration space should specify all possible connectivities among the N sites which constitute a unit of the transfer matrix, namely, a cross section of the transfer-matrix bar; see Fig. 1. In the figure, we also presented a drawing of an example of connectivity among the $N=4$ sites.

As shown in the figure, an integer index $\alpha=1,2,\dots,N$ specifies the position of the constituent sites of a transfer-matrix unit. In other words, the transfer-matrix unit is of one-dimensional structure rather than a two-dimensional one. Such a feature might be confusing, compared with the drawing in Fig. 1(a), where the transfer-matrix unit is drawn as a rectangular shape with the edges \sqrt{N} . Actually, the dimensionality is lifted to $d=2$ afterward by introducing the \sqrt{N} th-neighbor long-range interactions among the N sites. We will explain this scheme explicitly in Sec. II B. Here, for the

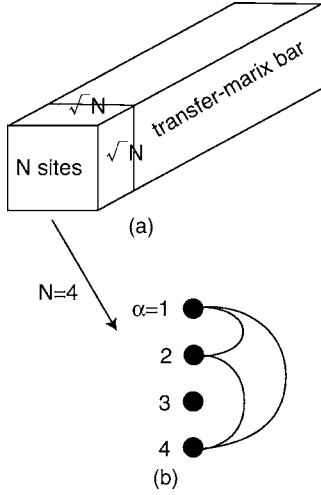


FIG. 1. (a) A drawing of the transfer-matrix bar. A unit of the transfer-matrix slice consists of N sites. (b) An example of connectivity among the $N(=4)$ sites. Such a connectivity is represented by the matrix notation, Eq. (2).

time being, we consider that these N sites are arranged into a one-dimensional structure.

In order to specify the connectivity among the N sites, we accepted the following matrix-based representation:

$$[a_i]_{\alpha\beta} = \begin{cases} 1 & \text{for a pair of connected sites } (\alpha, \beta) \\ 0 & \text{otherwise} \end{cases}. \quad (1)$$

The index i runs over all possible connectivities among the N sites. For example, the connectivity of Fig. 1(b) is represented by

$$a = \begin{pmatrix} 1 & 1 & 0 & 1 \\ 1 & 1 & 0 & 1 \\ 0 & 0 & 1 & 0 \\ 1 & 1 & 0 & 1 \end{pmatrix}. \quad (2)$$

Let us mention a few remarks: The authors in Ref. [1], accepted a more elaborated representation scheme. Namely, they specified whether a cluster is connected with the ‘‘origin’’ or that a cluster is an isolated one. Here, the origin stands for an edge of the transfer-matrix bar. An advantage of their extended representation is that one only needs to evaluate the largest eigenvalue of the transfer matrix to obtain the correlation length. Here, however, we did not accept their representation scheme. Correspondingly, we calculated the subdominant eigenvalue together with the dominant one in order to calculate the correlation length. This task is not so computationally demanding, and it renders significant simplification of the formalism mentioned below.

B. Explicit formula of the transfer-matrix elements for the $d=3$ bond percolation

In this section, we present the explicit formula for the transfer-matrix elements. We consider an anisotropic bond percolation on the cubic lattice. Namely, we set the percolation probabilities p_{\parallel} , $p_{\perp 1}$ and $p_{\perp 2}$ independently for the re-

spective bond directions along the $d=3$ Cartesian axes. Correspondingly, we factorize the transfer matrix into the following three components:

$$T = T_{\perp}(v, p_{\perp 2}) T_{\perp}(1, p_{\perp 1}) T_{\parallel}(p_{\parallel}) \quad (3)$$

with

$$v = \sqrt{N}. \quad (4)$$

(We followed the idea of Derrida and Vannimenus, who decomposed the transfer matrix for the $d=2$ percolation into two factors [1].) The components $T_{\parallel}(p_{\parallel})$, $T_{\perp}(1, p_{\perp 1})$, and $T_{\perp}(v, p_{\perp 2})$ denote the transition probabilities due to the longitudinal bond, intracluster nearest-neighbor bond, and the intracluster v th-neighbor bond, respectively. (Here, the ‘‘cluster’’ stands for the N sites constituting a unit of the transfer-matrix slice, and the ‘‘longitudinal’’ direction is parallel to the transfer-matrix bar; see Fig. 1.)

In other words, the product of two components $T_{\parallel}(p_{\parallel}) T_{\perp}(1, p_{\perp 1})$, namely, with $T_{\perp}(v, p_{\perp 2})$ ignored, should yield the transfer matrix for the $d=2$ bond percolation. The remaining factor $T_{\perp}(v, p_{\perp 2})$ lifts the dimensionality to $d=3$.

We present the explicit formulas for each component. First, for simplicity, we consider the longitudinal part T_{\parallel} . (This is essentially the same as the horizontal factor M_H appearing in the formalism [1] for the $d=2$ percolation.) Our formula for the elements of T_{\parallel} is given by

$$[T_{\parallel}(p_{\parallel})]_{ij} = \sum_{\{J_{\alpha}\}} p(\{J_{\alpha}\}, p_{\parallel}) (a_i, m(\{J_{\alpha}\}) \otimes a_j). \quad (5)$$

Here, the summation $\sum_{\{J_{\alpha}\}}$ runs over all possible random-bond configurations $\{J_{\alpha}\}$ with either $J_{\alpha}=0$ (unoccupied bond) or 1 (occupied bond) for $\alpha=1, 2, \dots, N$. The probability $p(\{J_{\alpha}\}, p_{\parallel})$ is given by

$$P(\{J_{\alpha}\}, p_{\parallel}) = p_{\parallel}^{N_{J=1}} (1 - p_{\parallel})^{N - N_{J=1}} \quad (6)$$

with the number of occupied bonds $N_{J=1}$. The ‘‘random-bond’’ matrix $m(\{J_{\alpha}\})$ is a diagonal $N \times N$ matrix with the diagonal elements $[m(\{J_{\alpha}\})]_{\beta\beta} = J_{\beta}$. The operation \otimes denotes the matrix product,

$$[a \otimes b]_{\alpha\beta} = \sum_{\gamma=1}^N ' a_{\alpha\gamma} \wedge b_{\gamma\beta}, \quad (7)$$

with the logical product \wedge in the Boolean algebra. (The summation Σ' gives 1, unless all the summands are zero.) The product (a_i, a_j) accounts for the orthogonality of the matrices; namely,

$$(a_i, a_j) = \delta_{ij}, \quad (8)$$

with Kronecker’s symbol δ_{ij} .

As would be apparent from the above formula (5), the transfer-matrix element $[T_{\parallel}]_{ij}$ stands for the transition probability from the initial configuration a_j to the final configuration a_i through the longitudinal random-bond percolation $\{J_{\alpha}\}$.

Second, we turn to considering the transverse component $T_{\perp}(w, p_{\perp})$. This component accounts for the intracluster w th-neighbor random-bond percolation with the percolation

probability p_{\perp} . This factor is the most significant part in our formalism. We propose the following formula for $T_{\perp}(w, p_{\perp})$:

$$[T_{\perp}(w, p_{\perp})]_{ij} = \sum_{\{J_{\alpha\beta}\}} p(\{J_{\alpha\beta}\}, p_{\perp}) t_{ij}(w, \{J_{\alpha\beta}\}). \quad (9)$$

The transition amplitude t_{ij} is given by

$$t_{ij}(w, \{J_{\alpha\beta}\}) = \sum_{\beta=1}^N f_{\beta}(w) (a_i, m_{\beta}(\{J_{\alpha\beta}\}) \oplus a_j). \quad (10)$$

Here, the symbol \oplus denotes an operation,

$$[a \oplus b]_{\alpha\beta} = \sum_{\gamma=1}^N 'a_{\alpha\gamma} \vee b_{\gamma\alpha}, \quad (11)$$

with the logical summation \vee in the Boolean algebra. The “ β th-neighbor-random-bond matrix” $m_{\beta}(\{J_{\alpha\beta}\})$ is given by the formula,

$$m_{\beta}(\{J_{\alpha\beta}\}) = m(\{J_{\alpha\beta}\}) \otimes s_{\beta}, \quad (12)$$

with the shift operator,

$$[s_{\beta}]_{\gamma\delta} = \begin{cases} 1 & \text{for } \gamma - \delta = \beta \bmod N \\ 0 & \text{otherwise} \end{cases}. \quad (13)$$

The operation s_{β} shifts the diagonal random-bond operator $m(\{J_{\alpha\beta}\})$ to an off-diagonal one, which now represents the β th-neighbor random bonds. That is, the operation $m_{\beta}(\{J_{\alpha\beta}\}) \oplus a_j$ introduces new intracluster β th-neighbor-random-bond percolation in adding to the initial connectivity a_j .

In order to implement the w th-neighbor intracluster percolation with a nonintegral value of w , we need to average over all sectors $\beta=1, 2, \dots, N$ with an appropriate weight $f_{\beta}(w)$; see Eq. (10). We propose that the weight should be given by the w th-order power of the shift operator

$$f_{\beta}(w) = [(s_1)^w]_{1\beta}. \quad (14)$$

As would be apparent from the definition, the operator $(s_1)^w$ generates the translational shift of the distance w , and the factor $f_{\beta}(w)$ picks up the amplitude of each sector β . Hence, the resulting formula, Eq. (10), should be the transition amplitude from a_j to a_i by the w th-neighbor random-bond percolation. Hence, the product $T_{\perp}(v, p_{\perp 2}) T_{\perp}(1, p_{\perp 1})$ with $v = \sqrt{N}$ introduces a two-dimensional intracluster percolation among the N sites. As noted previously, a crucial point is that there is no restriction to the number of constituent sites N .

Lastly, let us argue a conceptual difference from the original Novotny method [4] for the Ising ferromagnet. In the original method, the translation operator $(s_1)^w$ acts on the configuration space, which has huge dimensionality. On the contrary, in our formalism, the operator $(s_1)^w$ is a mere $N \times N$ matrix. Hence, from the viewpoint of the computer programming, the present formalism for the percolation is even simpler than the original method. (Here, the generation of the list of connectivity $\{a_j\}$ is the most time-consuming.)

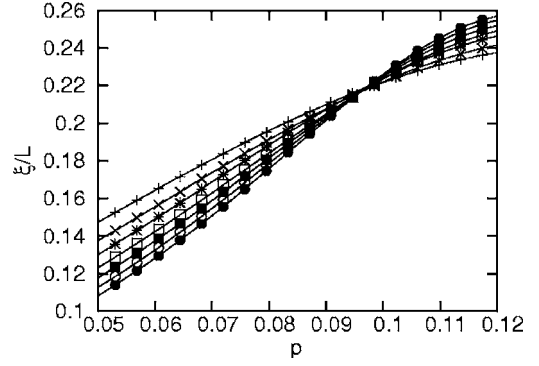


FIG. 2. The scaled correlation length ξ/L is plotted for the percolation probability p with the fixed anisotropy parameter $R=3.3$. The symbols $+$, \times , $*$, \square , \blacksquare , \circ , and \bullet denote the system sizes $N=4, 5, 6, 7, 8, 9$, and 10 , respectively; note that the relation $L=\sqrt{N}$ holds. From the intersection point of these curves, we read off the location of the critical point (percolation threshold) as $p_c \approx 0.096$.

III. NUMERICAL RESULTS

In Sec. II, we set up the transfer-matrix formalism for the $d=3$ bond percolation. In this section, we present the numerical results by means of the exact diagonalization of the transfer matrix. We consider the anisotropic bond percolation. The anisotropy parameter R governs the mutual ratios of the percolation probabilities; namely,

$$R^{-1} p_{\parallel} = R^{-1} p_{\perp 1} = p_{\perp 2} = p. \quad (15)$$

We consider the anisotropy ratio R as a freely tunable parameter to stabilize the finite-size corrections. Diagonalizing the system sizes $N=4, 5, \dots, 10$, we analyze the percolation transition in terms of the phenomenological renormalization group [2] method. Note that the linear dimension of the system L is given by the relation,

$$L = \sqrt{N}, \quad (16)$$

as shown in Fig. 1.

A. Percolation threshold p_c

In Fig. 2, we plotted the scaled correlation length ξ/L for the percolation probability p with the fixed anisotropy parameter $R=3.3$. (Afterward, we explain how we adjusted the anisotropy parameter to $R=3.3$.) The symbols $+$, \times , $*$, \square , \blacksquare , \circ , and \bullet denote the system sizes $N=4, 5, 6, 7, 8, 9$, and 10 , respectively. The correlation length ξ is calculated by the formula $\xi=1/\ln(\lambda_1/\lambda_2)$ with the dominant λ_1 and the subdominant λ_2 eigenvalues of the transfer matrix.

The intersection point of the curves in Fig. 2 indicates the location of the critical point (percolation threshold) p_c . (The scaled correlation length ξ/L is invariant with respect to the system size N at $p=p_c$.) Hence, we observe that a percolation transition occurs around $p \approx 0.096$.

In order to determine the critical point p_c more precisely, in Fig. 3, we plotted the approximate transition point $p_c(L_1, L_2)$ for $[2/(L_1+L_2)]^2$. Here, the approximate transition point $p_c(L_1, L_2)$ denotes the location of the intersection point

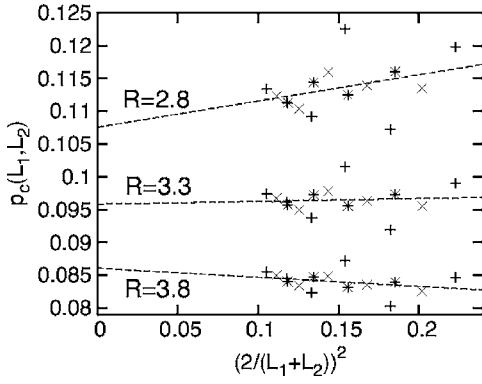


FIG. 3. The approximate critical point $p_c(L_1, L_2)$ is plotted for $[2/(L_1+L_2)]^2$ and the various values of the anisotropy parameter $R=2.8, 3.3,$ and 3.8 . The symbols $+$, \times , and $*$ denote the differences of the system sizes $N_1-N_2=1, 2,$ and 3 , respectively. We also presented the slopes with the least-squares fit to the data as the dashed lines. We see that the finite-size corrections to p_c are suppressed on setting $R=3.3$.

of the curves for a pair of (L_1, L_2) . The symbols $+$, \times , and $*$ show that the differences of the system sizes are $N_1-N_2=1, 2,$ and 3 , respectively; note that the relation $L_{1,2}=\sqrt{N_{1,2}}$ holds. As indicated in Fig. 3, we survey several values of the anisotropy parameter such as $R=2.8, 3.3,$ and 3.8 . Thereby, we notice that the finite-size corrections to p_c are suppressed on setting $R=3.3$. The least-squares fit to the data for $R=3.3$ yields the critical point $p_c=0.0958(27)$ in the thermodynamic limit $L\rightarrow\infty$.

Let us argue the role of the anisotropy parameter R . First of all, it is worthwhile that the system size along the transfer-matrix (longitudinal) direction is infinite, whereas the transverse system sizes are both finite $L\leq\sqrt{10}$; see Fig. 1. In this sense, it is by no means necessary to consider the isotropic condition $p_{\perp 1}=p_{\perp 2}=p_{\parallel}$ specifically. Hence, we consider that the ratio $R=p_{\parallel}/p_{\perp 2}$ is a tunable parameter. Practically, we found that the finite-size corrections improve for large R . Second, we need to remedy the dimensionality $d=3$ by adjusting the ratio of the intracluster interactions $R=p_{\perp 1}/p_{\perp 2}$. That is, the “effective dimension” [5,6] can deviate slightly from $d=3$, at least, for small system sizes. (This deviation deteriorates the finite-size-scaling analysis.) Note that basically, the backbone structure of Novotny’s transfer matrix is of $d=2$, and the dimensionality is lifted to $d=3$ by introducing the long-range interactions among the intracluster sites. In other words, it is not quite obvious that the dimensionality $d=3$ is realized precisely, at least, for small N . Hence, in order to remedy this dimensionality deviation, we should tune [5,9] the intracluster-interaction ratio $R=p_{\perp 1}/p_{\perp 2}$. [Note that for large R , the component $T_{\perp}(1, p_{\perp 1})$ dominates $T_{\perp}(v, p_{\perp 2})$, and the dimensionality reduces to $d=2$. For a certain moderate value of R , the dimensionality would approach $d=3$.] More specifically, we adjusted R so as to improve the finite-size-scaling behaviors of $p_c(L_1, L_2)$ [5,6] as shown in Fig. 3. In this respect, there might exist alternative parametrization schemes other than the present one. Here, however, we accepted the simplest parametrization scheme $p_{\parallel}=p_{\perp 1}=Rp_{\perp 2}$ involving a single tunable parameter R .

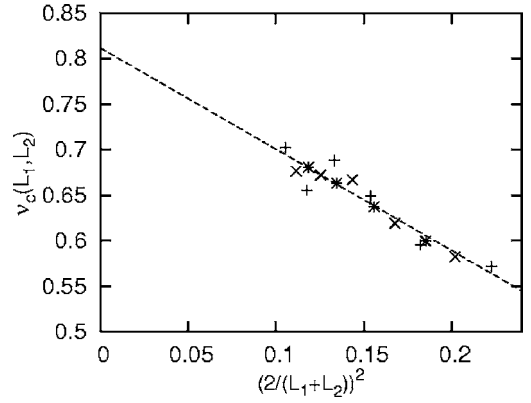


FIG. 4. The approximate correlation-length critical exponent $\nu(L_1, L_2)$ is plotted for $[2/(L_1+L_2)]^2$ with the fixed anisotropy parameter $R=3.3$. The symbols $+$, \times , and $*$ denote the differences of the system sizes $N_1-N_2=1, 2,$ and 3 , respectively. The least-squares fit to these data yields $\nu=0.812(15)$ in the limit $L\rightarrow\infty$.

B. Correlation-length critical exponent ν

In this section, we study the criticality at $p=p_c$. In Fig. 4, we plotted the approximate correlation-length critical exponent [2],

$$\nu(L_1, L_2) = \ln(L_1/L_2) \left/ \ln \left(\frac{\partial[\xi(L_1)/L_1]}{\partial p} / \frac{\partial[\xi(L_2)/L_2]}{\partial p} \right) \right|_{p=p_c}, \quad (17)$$

for $[2/(L_1+L_2)]^2$. Here, we set $p_c=0.0958$ and $R=3.3$. The symbols $+$, \times , and $*$ show that the differences of the system sizes are $N_1-N_2=1, 2,$ and 3 , respectively. Note that this formula contains a p derivative, which is readily calculated with the transfer-matrix method very precisely. (The transfer-matrix data are free from the statistical error.)

We see that the data align rather satisfactorily. The least-squares fit to these data yields an extrapolated value $\nu=0.812(15)$ to the thermodynamic limit $L\rightarrow\infty$. Similarly, we obtain $\nu=0.813(21)$ by omitting the $L=10$ data. Thereby, we confirm that the data are almost converged.

In order to check the reliability of ν further, we try to manage alternative extrapolation schemes: First, we replace the abscissa in Fig. 3 with the refined one $[2/(L_1+L_2)]^{\omega+1/\nu}$ [10], where we used $\omega=1.61(5)$ and $\nu=0.89(2)$ reported in Ref. [11]. Thereby, we arrive at $\nu=0.811(15)$. This result indicates the stability of ν with respect to p_c . Second, replacing the abscissa in Fig. 4 with $[2/(L_1+L_2)]^{\omega}$, we obtain $\nu=0.853(19)$. Actually, this refined extrapolation yields an “improved” value for ν . However, for the sake of self-consistency, we do not accept this refined extrapolation method and consider it as a reference. Lastly, setting the values of the anisotropy parameter as $R=2.8$ and $R=3.8$, we obtain $\nu=0.853(27)$ and $\nu=0.771(11)$, respectively. These results again confirm the stability of ν satisfactorily.

Recollecting these results, we estimate the correlation-length critical exponent as,

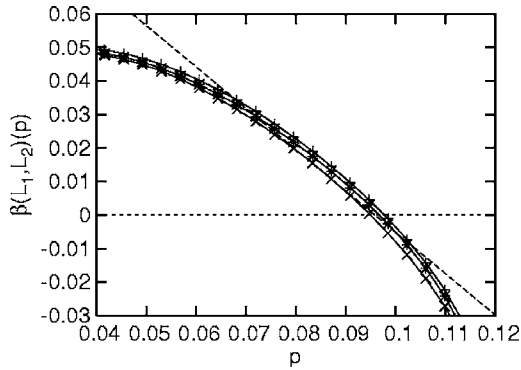


FIG. 5. The approximate beta function $\beta(L_1, L_2)$ (19) is plotted for the percolation probability p with the fixed anisotropy parameter $R=3.3$. The symbols $+$, \times , and $*$ show that the pairs of the system sizes are $(N_1, N_2)=(6, 8)$, $(7, 9)$, and $(8, 10)$, respectively. We also presented a slope $-(p-p_c)/\nu$ with $p_c=0.0958$ and $\nu=0.812$ determined in Figs. 3 and 4.

$$\nu = 0.81(5), \quad (18)$$

with an expanded error margin.

Let us recollect a number of recent estimates for ν determined with other approaches: From the series expansion method, Dunn *et al.* [12] obtained $\nu=0.83(5)$. On the other hand, the Monte Carlo studies have reported $\nu=0.89(2)$ [11], $\nu=0.8765(16)$ [13], $\nu=0.893(40)$ [14], and $\nu=0.868(11)$ [15]. These estimates and ours are consistent with each other within the error margins. Nevertheless, we stress that our motivation is not necessarily directed to the accurate estimation of the critical indices. In Sec. IV, we address an extended remark on the potential applicability of our scheme and future perspective.

Lastly, in Fig. 5, we present the approximate β function [16],

$$\beta(L_1, L_2) = \frac{1 - \ln[\xi(L_1)/\xi(L_2)]/\ln(L_1/L_2)}{\sqrt{\frac{\partial \xi(L_1)}{\partial p} \frac{\partial \xi(L_2)}{\partial p} / \xi(L_1)/\xi(L_2)}}, \quad (19)$$

for $R=3.3$. (Note that this formula also contains the derivatives, and it is hardly accessible by other approaches.) The symbols $+$, \times , and $*$ show that the pairs of system sizes are $(N_1, N_2)=(6, 8)$, $(7, 9)$, and $(8, 10)$, respectively. The beta function provides rich information on the overall feature of the criticality. The zero point $\beta(p)|_{p=p_c}=0$ indicates the location of the transition point p_c , and the slope at the transition point yields the inverse of ν . In the figure, we presented a slope $-(p-p_c)/\nu$ with $p_c=0.0958$ and $\nu=0.81$ determined above. The slope well describes the behavior of the beta function in the vicinity of $p=p_c$. However, in a closer look, the beta function bends convexly, indicating that non-negligible corrections to scaling do exist. Possibly, such severe corrections are reflected in Fig. 4, where we observe pronounced finite-size corrections to ν . However, these corrections are fairly systematic so that we could manage the extrapolation to $L \rightarrow \infty$ rather unambiguously. This is an advantage of Novotny's method, with which a variety of sys-

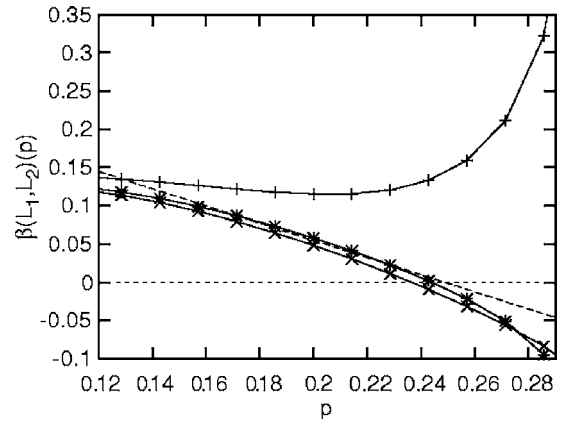


FIG. 6. The approximate beta function $\beta(L_1, L_2)$ (19) is plotted for the percolation probability p at $R=1$ (isotropic point). The symbols $+$, \times , and $*$ show that the pairs of the system sizes are $(N_1, N_2)=(6, 8)$, $(7, 9)$, and $(8, 10)$, respectively. We also presented a slope $-(p-p_c)/\nu$ with $p_c=0.248\ 812\ 6$ and $\nu=0.89$ reported in Ref. [11] as a dashed line.

tem sizes are available even for the case of $d=3$.

C. Isotropic case $p_{\parallel}=p_{\perp 1}=p_{\perp 2}$

In Fig. 6, we plotted the beta function $\beta(L_1, L_2)$ for $R=1$ (isotropic case). The symbols $+$, \times , and $*$ show that the pairs of system sizes are $(N_1, N_2)=(6, 8)$, $(7, 9)$, and $(8, 10)$, respectively. We also presented a slope $-(p-p_c)/\nu$ with $p_c=0.248\ 812\ 6$ and $\nu=0.89$ [11] as a dashed line. We see that our data and the slope behave similarly in the vicinity of $p=p_c$. We obtain the correlation-length critical exponent $\nu \approx 0.64$ from a pair of $N=8$ and 10 . However, for small N , the data scatter, and eventually, even the zero point of the beta function disappears. Because of this irregularity, we cannot manage systematic extrapolation to the thermodynamic limit. In this sense, the anisotropy parameter R is significant in order to stabilize the finite-size corrections of the transfer-matrix data as demonstrated in Secs. III A and III B.

IV. SUMMARY AND DISCUSSIONS

We developed a transfer-matrix formalism for the $d=3$ bond percolation. Our formalism is based on Novotny's idea [4], which has been applied to the Ising models in high dimensions $d \leq 7$. We demonstrated that his idea is also applicable to the $d=3$ bond percolation. A key ingredient of his method is that we can treat an arbitrary number of sites constituting a unit of the transfer-matrix slice; see Fig. 1.

Diagonalizing the transfer matrix for the system sizes $N=4, 5, \dots, 10$, we studied the criticality of the percolation transition. We found that the numerical data are well described by the finite-size-scaling theory, and thereby, we obtained an estimate for the correlation-length critical exponent $\nu=0.81(5)$. Here, we tuned the anisotropy parameter to $R=3.3$ in order to reduce the finite-size corrections. Because the system size along the transfer-matrix direction is infinite, it is by no means necessary to consider the isotropic limit $R=1$ specifically.

The aim of this paper is to demonstrate an applicability of the transfer-matrix method to the geometrical problem such as the percolation *even for* $d=3$. As mentioned in the introduction, the transfer-matrix method has some advantages over the Monte Carlo method. Actually, as for the $d=2$ percolation, the transfer-matrix approach [17] has made a unique contribution, although its accuracy as to the critical indices is not particularly superior to that of Monte Carlo. Lastly, let us address a remark on the advantage of our approach: For example, according to Fortuin and Kasteleyn [18], the q -state Potts model admits a geometrical representation in terms of the bond percolation. Namely, based on the percolation framework, one is able to extend the integral number q to a continuously variable one. In fact, in $d=3$, an extensive Monte Carlo study [19] reports an existence of the critical value $q_c=2.45(10)$, above which the magnetic transition becomes discontinuous; see also Ref. [20]. However, the nature of this singularity is not fully understood, because the Monte Carlo method cannot deal with the complex- q number

(due to the negative sign problem). On the contrary, *the transfer-matrix method is free this difficulty*. Actually, with the transfer-matrix method, in $d=2$, in the complex- q plane, the distribution of zeros (of the partition function) was investigated [21–23]. As for $d=3$, however, similar consideration has not yet been done due to the lack of an efficient algorithm. Our scheme meets such a requirement. Moreover, the low-lying spectrum of the Potts model in $d=3$ is of fundamental significance [24], and the problem also remained unsolved. In this sense, our scheme provides a step toward a series of such longstanding problems, to which the Monte Carlo method does not apply. An effort toward this direction is in progress, and it will be addressed in future study.

ACKNOWLEDGMENTS

This work is supported by a Grant-in-Aid for Young Scientists (No. 15740238) from Monbukaagakusho, Japan.

-
- [1] B. Derrida and J. Vannimenus, *J. Phys. (Paris), Lett.* **41**, L473 (1980).
 [2] M. P. Nightingale, *Physica A* **83**, 561 (1976).
 [3] D. Stauffer and A. Aharony, *Introduction to Percolation Theory* (Taylor and Francis, London, 1994).
 [4] M. A. Novotny, *J. Appl. Phys.* **67**, 5448 (1990).
 [5] M. A. Novotny, *Phys. Rev. B* **46**, 2939 (1992).
 [6] M. A. Novotny, *Phys. Rev. Lett.* **70**, 109 (1993).
 [7] M. A. Novotny, *Computer Simulation Studies in Condensed Matter Physics III*, edited by D. P. Landau, K. K. Mon and H-B. Schüttler (Springer-Verlag, Berlin, 1991).
 [8] Y. Nishiyama, *Phys. Rev. E* **70**, 026120 (2004).
 [9] Y. Nishiyama, *Phys. Rev. E* **71**, 046112 (2005).
 [10] K. Binder, *Z. Phys. B: Condens. Matter* **43**, 119 (1981).
 [11] C. D. Lorenz and R. M. Ziff, *Phys. Rev. E* **57**, 230 (1998).
 [12] A. G. Dunn, J. W. Essam, and D. S. Ritchie, *J. Phys. C* **8**, 4219 (1975).
 [13] H. G. Ballesteros, L. A. Fernández, V. Marin-Mayor, A. Muñoz Sudupe, G. Parisi, and J. J. Ruiz-Lorenzo, *J. Phys. A* **32**, 1 (1999).
 [14] Y. Tomita and Y. Okabe, *J. Phys. Soc. Jpn.* **71**, 1570 (2002).
 [15] P. H. L. Martins and J. A. Plascak, *Phys. Rev. E* **67**, 046119 (2003).
 [16] H. H. Roomany and H. W. Wyld, *Phys. Rev. D* **21**, 3341 (1980).
 [17] H. W. J. Blöte and M. P. Nightingale, *Physica A* **112**, 405 (1982).
 [18] C. M. Fortuin and P. W. Kasteleyn, *Physica (Amsterdam)* **57**, 536 (1972).
 [19] J. Lee and J. M. Kosterlitz, *Phys. Rev. B* **43**, R1268 (1991).
 [20] F. Gliozzi, *Phys. Rev. E* **66**, 016115 (2002).
 [21] S-Y. Kim, R. J. Creswick, C-N. Chen, and C-K. Hu, *Physica A* **281**, 262 (2000).
 [22] S-Y. Kim and R. J. Creswick, *Phys. Rev. E* **63**, 066107 (2001).
 [23] S-C. Chang and R. Shrock, *Phys. Rev. E* **64**, 066116 (2001).
 [24] J-D. Wang and C. DeTar, *Phys. Rev. D* **47**, 4091 (1993).